Applied Catalysis A: General 502 (2015) 361–369

Contents lists available at ScienceDirect

Applied Catalysis A: General

journal homepage: www.elsevier.com/locate/apcata

Kinetics and site requirements of ether disproportionation on γ-Al_2O_3

Joseph F. DeWilde, Aditya Bhan*

Department of Chemical Engineering and Materials Science, University of Minnesota—Twin Cities, 421 Washington Avenue SE, Minneapolis, MN 55455, USA

ARTICLE INFO

Article history:
Received 30 April 2015
Received in revised form 5 June 2015
Accepted 7 June 2015
Available online 19 June 2015

Keywords:
Ether disproportionation
Alkenes
Kinetics
γ-Alumina
Site requirements

ABSTRACT

Measured rates of methyl propyl ether (MPE), an asymmetric ether, conversion on γ-alumina at 623 K verify that hydration rates are negligible compared to disproportionation rates below 2.0 kPa of water.

Steady state kinetic measurements establish that diethyl ether (DEE) disproportionation rates possess reaction orders between 0 and 1. A mechanism for DEE disproportionation in which ethanol monomers and reactive ethoxy species are the primary surface species is consistent with measured pressure dependencies. The intrinsic rate constant of DEE disproportionation is nearly identical to that of unimolecular ethanol dehydration, revealing the similarity in the rate-limiting steps of these two reactions. In-situ pyridine titration studies verify that DEE disproportionation and unimolecular ethanol dehydration possess similar site requirements and densities (0.3 and 0.2 sites nm^{-2}, respectively) while bimolecular ethanol dehydration occurs on a separate pool of catalytic sites.

1. Introduction

Alcohols dehydrate over acid catalysts, such as gamma-alumina (γ-Al_2O_3) [1–7], to form olefins and water through a unimolecular pathway or ethers and water through a bimolecular pathway [8–21]. In previous investigations, pyridine inhibition measurements identified that these parallel alcohol dehydration pathways occur on non-equivalent pools of catalytic sites. Concurrently, kinetic measurements have demonstrated that, at 488 K, alcohol dehydration is inhibited by non-reactive multimers while at temperatures greater than 623 K the surface is primarily covered with reactive precursors [22–24]. Specifically, olefin production from the dehydration of ethanol, 1-propanol, isopropanol, and isobutanol at 488 K was observed to be inhibited by surface dimers composed of alcohol and water while ether synthesis was inhibited by surface trimer species at alcohol pressures larger than 4.2 kPa [24]. The proposed presence of surface multimers at low temperatures is consistent with kinetic measurements of propylene synthesis from 2-propanol dehydration at 373–433 K by De Morgues et al. [25] which demonstrated that the rate of propylene synthesis was independent of 2-propanol pressure above 1.1 kPa while simultaneously being inhibited by co-fed water at water partial pressures below 1.2 kPa. In addition to alcohol dehydration, ethers can also convert on γ-Al_2O_3 through two possible reaction pathways: (i) ether hydration, the reverse reaction pathway of bimolecular alcohol dehydration, and (ii) direct ether disproportionation to form an olefin and an alcohol [26–29]. In this work, we identify the prominent ether conversion pathway at 623 K as well as elucidate its kinetics (including the prominent surface species present during reaction) and mechanism.

Negligible quantities of ether were observed from ethanol reactions at 623 K on γ-Al_2O_3 at conversions greater than 99% in investigations by Phung et al. [26], suggesting that ether conversion pathways exist on γ-Al_2O_3. This observation is consistent with ethanol dehydration measurements presented in Fig. S1 in which diethyl ether (DEE) selectivity over γ-Al_2O_3 at 623 K decreases with increasing space time before becoming negligible at ethanol conversions of ~99%. Reactor effluent DEE partial pressure was observed to go through a maximum with increasing contact time over a bed of γ-Al_2O_3 at 571 and 616 K in steady state kinetic measurements of ethanol dehydration by Knözinger and Köhne [27]. The authors additionally observed that ethylene and ethanol were synthesized in a nearly 1:1 stoichiometric ratio at <10% conversion in kinetic measurements of ether conversion as a function of increasing temperature, and thus conversion, leading them to postulate that ether disproportionation presents a significant ether decomposition pathway on γ-Al_2O_3 [27]. The 1:1 stoichiometric production of ethylene and ethanol from DEE conversion on γ-Al_2O_3 was also observed in more recent investigations at 573 K by Phung and Busca [28]. Similarly, Morávek and Kraus [29] observed nearly equal steady state production of ethylene and ethanol with a much smaller production rate of water from the conversion of DEE on alumina at 523 K, consistent with a prominent ether

* Corresponding author. Fax: +1 612 626 7246.
E-mail addresses: dewil005@umn.edu (J.F. DeWilde), abhan@umn.edu (A. Bhan).

http://dx.doi.org/10.1016/j.apcata.2015.06.008
0926-860X/

disproportionation pathway on alumina materials. Furthermore, ethylene synthesis persisted after the DEE feed was stopped, leading the authors to infer that ether disproportionation occurs through the formation of persistent surface alkoxides that desorb to form ethylene [29]. In more recent investigations, density functional theory (DFT) calculations by Christiansen et al. [30] show that DEE disproportionates on the γ-Al_2O_3 surface with an activation energy nearly identical to that of ethylene synthesis from ethanol dehydration (38 and 37 kcal mol^{-1}, respectively), consistent with the authors' proposal that the rate-limiting step for the two reactions is similar.

DFT calculations (PW 91 functional) of the adsorption and dissociation energies of water on a variety of surface sites on γ-Al_2O_3 by both Wischert et al. [31] and Digne et al. [32] noted that these energies were dependent on the coordination of the surface aluminum atom and facet onto which the water molecule adsorbed, demonstrating that the surface of γ-Al_2O_3 possesses a distribution of active sites with varying acidities. Hendriksen et al. [33] noted that heats of water immersion on alumina samples outgassed at different temperatures (100–600 °C) decreased as the surface hydration of the alumina surface increased, consistent with these computational results. The presence of a distribution in acid site strength was also experimentally observed in both (i) infrared spectroscopic measurements by Morterra and Magnacca [34] as well as independently by Parry [35] and (ii) in ^{15}N nuclear magnetic resonance measurements by Ripmeester [36] of pyridine-exposed γ-Al_2O_3 samples in which multiple (i) vibrational bands around 1450 cm^{-1} and (ii) peaks with chemical shifts 110 and 134 ppm were attributed to pyridine adsorption onto Lewis acid sites of varying strengths. Similarly, multiple infrared vibrational bands (2238, 2200, and 2165 cm^{-1}) on CO-exposed γ-Al_2O_3 samples measured by Zecchina et al. [37] verify the non-uniformity of the γ-Al_2O_3 surface. Wischert et al. [38] further supported these conclusions with $^1\{H\}^{27}Al$ cross-polarization nuclear magnetic resonance measurements in which a range of both the measured chemical shift (between 10 and 70 ppm) and quadropolar coupling constants (between 5 and 38 MHz) were noted on γ-Al_2O_3 samples that were treated in synthetic air at 573 and 773 K. The area of a peak at ~23 ppm attributed to penta-coordinated aluminum atoms was observed to decrease with BaO loading in ^{27}Al nuclear magnetic resonance measurements by Kwak et al. [16] on BaO/γ-Al_2O_3; peaks attributed to octahedral (0 ppm reference in this study) and tetrahedral (~59 ppm) aluminum atoms were unaffected by the BaO loading. The rate of methanol dehydration to synthesize DME decreased monotonically with BaO loading on these catalytic systems [18], suggesting that these penta-coordinated sites on γ-Al_2O_3 are active for ether synthesis. While olefin synthesis was not investigated in these studies, these experiments suggest that multiple types of potential catalytic sites exist on γ-Al_2O_3. The diversity and number of acid sites is expected to be a function of temperature and water partial pressure and, based on our prior reports, results in at least two distinct sets of catalytic centers, one which catalyze unimolecular alcohol dehydration and dehydrogenation reactions and another which catalyzes bimolecular alcohol dehydration reactions [22,23]. We report in this study that ether disproportionation occurs on sites that catalyze unimolecular alcohol conversion.

In this investigation, kinetic measurements of methyl propyl ether (MPE), an asymmetric ether, verify that ether disproportionation, rather than ether hydration, is the predominant ether conversion pathway on γ-Al_2O_3 at water partial pressures below 2.0 kPa. Measured DEE disproportion rates are independent of co-fed water partial pressure and are consistent with a proposed mechanism in which reactive DEE-derived ethoxy groups and inhibitory ethanol monomers are the prominent surface species. In-situ pyridine inhibition experiments are used to affirm that the catalytic sites responsible for DEE disproportionation possess similar site requirements and densities (0.3 and 0.2 sites nm^{-2}, respectively) as ethylene synthesis from ethanol dehydration.

2. Experiments

2.1. Catalyst preparation

Kinetic measurements were carried out on γ-Al_2O_3 purchased from the manufacturer (18HPa-150Catalox, BET surface area = 141 m^2/g^{-1}, pore volume = 0.786 $cm^3\,g^{-1}$). Two batches of catalyst particles, one with particle sizes between 180 and 420 μm (40–80 mesh) for reactions of DEE, ethanol, and water mixtures and one with particle sizes between 180 and 250 μm (60–80 mesh) for measuring MPE kinetics and pyridine inhibition, were prepared by pressing and subsequently sieving γ-Al_2O_3 powder. The desired catalyst mass (~1.0 mg) was obtained by individually counting catalyst particles and adding them to a quartz tube reactor filled with acid-washed quartz sand as described in previous reports [22,23]. The catalyst beds were then treated in air and subsequently exposed to 2.2 kPa of water prior to reaction as described previously [23].

2.2. Steady state kinetic measurements

The reactor system described in previous reports [22,23] was used to gather steady state kinetic measurements on ether conversion. All experiments were performed at a reaction temperature of 623 K using a mixture of liquid feeds, a He carrier gas (Grade 4.7, Minneapolis Oxygen Company) with a flowrate of 9.9 $cm^3\,s^{-1}$ at ambient pressure, and a mixture of 25.0% CH_4 with a balance of Ar (Minneapolis Oxygen Company) fed at 0.017 $cm^3\,s^{-1}$ at ambient pressure to act as an internal standard for gas chromatography analysis. Ether conversions were kept to differential levels (<10%) by using reactor beds containing 1.0 mg of catalyst.

MPE (97% Sigma–Aldrich with 3% methanol as stabilizer) was fed to and vaporized in a flowing He stream to maintain a pressure of 0.8 kPa for kinetic measurements of asymmetric ether conversion. Methanol (99.9% Fisher Scientific) was also fed in these experiments to maintain a partial pressure of 0.2 kPa throughout the catalyst bed. Methanol and 1-PrOH dehydration kinetics were measured in independent investigations by feeding 2.4–16.8 kPa of methanol and 1.4–9.4 kPa of 1-PrOH (99.9% Sigma–Aldrich). Similarly, the kinetics of DEE conversion were measured by varying the partial pressure of ethanol-stabilized DEE (98.1% DEE with 1.8% ethanol Fisher Scientific) between 0.4 and 8.8 kPa. Pyridine inhibition measurements were carried out at 0.02–0.08 kPa of pyridine (99+%, Sigma–Aldrich) with a co-feed of non-stabilized DEE (99.9% Sigma–Aldrich) at 1.4 kPa as well as, in an independent experiment, a co-feed of 3.5 kPa of ethanol and 1.3 kPa of water. For all experiments used to evaluate alcohol and ether conversion kinetics as well as pyridine inhibition measurements, deionized water was co-fed to establish feed partial pressures between 0.2 and 2.1 kPa.

The composition of the reactor effluent was determined using an online gas chromatograph (GC) with previously described analytical protocols [22]. The 95% confidence intervals reported in tables and figures were evaluated from subsequent GC measurements at the same experimental conditions.

2.3. In-situ chemical titrations using pyridine

Steady state rates and transient profiles of the effluent composition during DEE conversion were measured using an online mass spectrometer on 0.005–0.010 g of γ-Al_2O_3 at 623 K and with a 1.5 kPa DEE feed upon the introduction of 0.02–0.05 kPa of pyridine to the feed. These profiles were used to determine the effective cat-

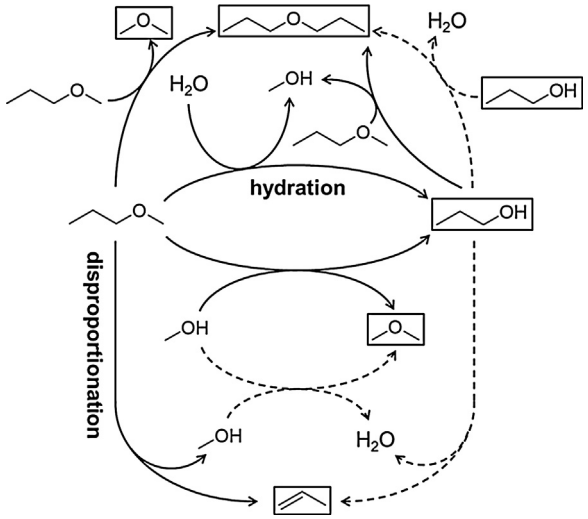

Scheme 1. Proposed reaction network for MPE conversion on γ-Al_2O_3. The effluent concentrations of compounds highlighted in boxes were measured experimentally, while the other compounds were fed to the reactor. The reactions indicated by dashed arrows signify reactions that were evaluated in independent kinetic measurements.

alyst mass that is active for DEE disproportionation in the reactor, as described previously for ethanol dehydration [23]. The density of active sites for DEE disproportionation was estimated by linearly extrapolating the inhibition profile and determining the surface density of pyridine necessary to completely deactivate the DEE disproportionation rate, as shown in previous reports [22–24].

2.4. Estimation of kinetic parameters

Bayesian statistical optimization techniques in the Athena Visual Studio statistical software package (v14.2, W. E. Stewart and M. Caracotsios) were employed to estimate reported kinetic parameters. Calculated 95% marginal highest posterior density intervals were used to determine the reported uncertainties. Independent measurements at the same reactant partial pressures acted as experimental replicates for parameter estimation.

3. Results and discussion

3.1. Kinetic measurements of MPE conversion

The product distribution of asymmetric ethers, such as MPE, allow for the rates of ether disproportionation to be deconvoluted from the rates of ether hydration because different products result from the two reactions. The hydration of MPE yields both methanol and propanol while MPE disproportionation will yield methanol and propylene. The rates of ether hydration, r_{hyd}, and ether disproportionation, r_{dis}, in a differential packed-bed reactor can therefore, be evaluated using Eqs. (1) and (2) (Scheme 1).

$$r_{hyd} = r_{PrOH} + r_{PrOHtoDPE} + r_{PrOH\,to\,C_3H_6} - r_{MPE+MeOH} - r_{MPE+PrOH} \quad (1)$$

$$r_{dis} = r_{C_3H_6} - r_{PrOH\ toC_3H_6} \quad (2)$$

$r_{C_3H_6}$ and r_{PrOH} represent the net rates of propylene and 1-propanol synthesis, respectively; $r_{PrOHtoDPE}$ and $r_{PrOHtoC_3H_6}$ are the rates of bimolecular and unimolecular 1-propanol dehydration to synthesize dipropyl ether (DPE) and propylene, respectively $r_{MPE+PrOH}$ denotes the rate of DPE and methanol formation from the reaction of MPE and 1-propanol; and $r_{MPE+MeOH}$ signifies the reaction rate of MPE and methanol to form dimethyl ether (DME) and 1-propanol. The rate of this reaction is given by Eq. (3).

$$r_{MPE+MeOH} = r_{DME} - r_{MeOHtoDME} - (r_{DPE} - r_{PrOHtoDPE} - r_{MPE+PrOH}) \quad (3)$$

r_{DME} and r_{DPE} are the net rates of DME and DPE synthesis, respectively; $r_{MeOHtoDME}$ represents the rate of methanol dehydration to synthesize DME. The term in the parentheses signifies the rate of DME formation from the reaction of two MPE molecules to form DPE and DME. The reaction sequence described in Eqs. (1)–(3) is shown in Scheme 1 and Eqs. (4)–(11).

$$C_3H_7OCH_3 + H_2O \rightarrow C_3H_7OH + CH_3OH \quad (4)$$

$$C_3H_7OCH_3 \rightarrow C_3H_6 + CH_3OH \quad (5)$$

$$C_3H_7OCH_3 + CH_3OH \rightarrow C_3H_7OH + CH_3OCH_3 \quad (6)$$

$$2C_3H_7OCH_3 \rightarrow C_3H_7OC_3H_7 + CH_3OCH_3 \quad (7)$$

$$2CH_3OH \rightarrow CH_3OCH_3 + H_2O \quad (8)$$

$$2C_3H_7OH \rightarrow C_3H_7OC_3H_7 + H_2O \quad (9)$$

$$C_3H_7OH \rightarrow C_3H_6 + H_2O \quad (10)$$

$$C_3H_7OH + C_3H_7OCH_3 \rightarrow C_3H_7OC_3H_7 + CH_3OH \quad (11)$$

Eqs. (1)–(3) contain three rates that can be evaluated in independent kinetic measurements: the unimolecular and bimolecular dehydration rates of 1-propanol to synthesize propylene and DPE, respectively, and the dehydration rate of methanol to DME.

The 1-propanol reaction order of the measured propylene synthesis rate from the unimolecular dehydration of 1-propanol on γ-Al_2O_3 at 623 K decreases from 0.6 to 0.4 as the 1-propanol pressure increases from 1.4 to 9.4 kPa (Fig. 1a). The reaction order of DPE synthesis from bimolecular 1-propanol dehydration also decreases with increasing alcohol partial pressure (decreasing from 1.7 to 0.7 between 1.4 and 9.4 kPa of 1-propanol; Fig. 1b). The methanol order of DME synthesis decreases from 0.9 to 0.7 as methanol pressure is increased from 2.4 to 15.8 kPa (Fig. 1c). All dehydration rates at 623 K were observed to be independent of water partial pressure at water partial pressures up to 2.3 kPa (Fig. 2).

The dehydration kinetics of 1-propanol and methanol match previous investigations of ethanol dehydration on γ-Al_2O_3 at 623 K in which dehydration rates were found to be consistent with a mechanism in which only reactive precursors (alcohol monomers for olefin synthesis and alcohol dimers for ether synthesis) cover the active sites during reaction [23]. The rate expressions shown in Eqs. (12) and (13) can be derived assuming that the reactive precursors prior to the rate-limiting step are the only prominent surface species and are in quasi-equilibrium with the alcohol in the vapor phase.

$$r_{olefin} = \frac{k_{olefin} K_{A1} P_{Alcohol}}{1 + K_{A1} P_{Alcohol}} \quad (12)$$

$$r_{ether} = \frac{k_{ether} K_{A1} K_{A2} P_{Alcohol}^2}{1 + K_{A1} K_{A2} P_{Alcohol}^2} \quad (13)$$

r_{olefin} and r_{ether} are the olefin and ether synthesis rates. k_{olefin} and k_{ether} signify the intrinsic rate constants for unimolecular and bimolecular alcohol dehydration, respectively. The equilibrium constant to form a surface alcohol monomer is signified by K_{A1} while K_{A2} represents the equilibrium constant for the adsorption of another alcohol molecule to the reactive monomer to form a surface alcohol dimer. $P_{Alcohol}$ represents the alcohol partial pressure in the catalyst bed. Table 1 summarizes the kinetic parameters of Eqs. (12) and (13) for 1-propanol and methanol dehydration estimated from the data presented in Figs. 1 and 2. Solid lines in Figs 1 and 2 show the models presented Eqs. (12) and (13) with the estimated kinetic parameters from Table 1. Figs. S2–S4 show the

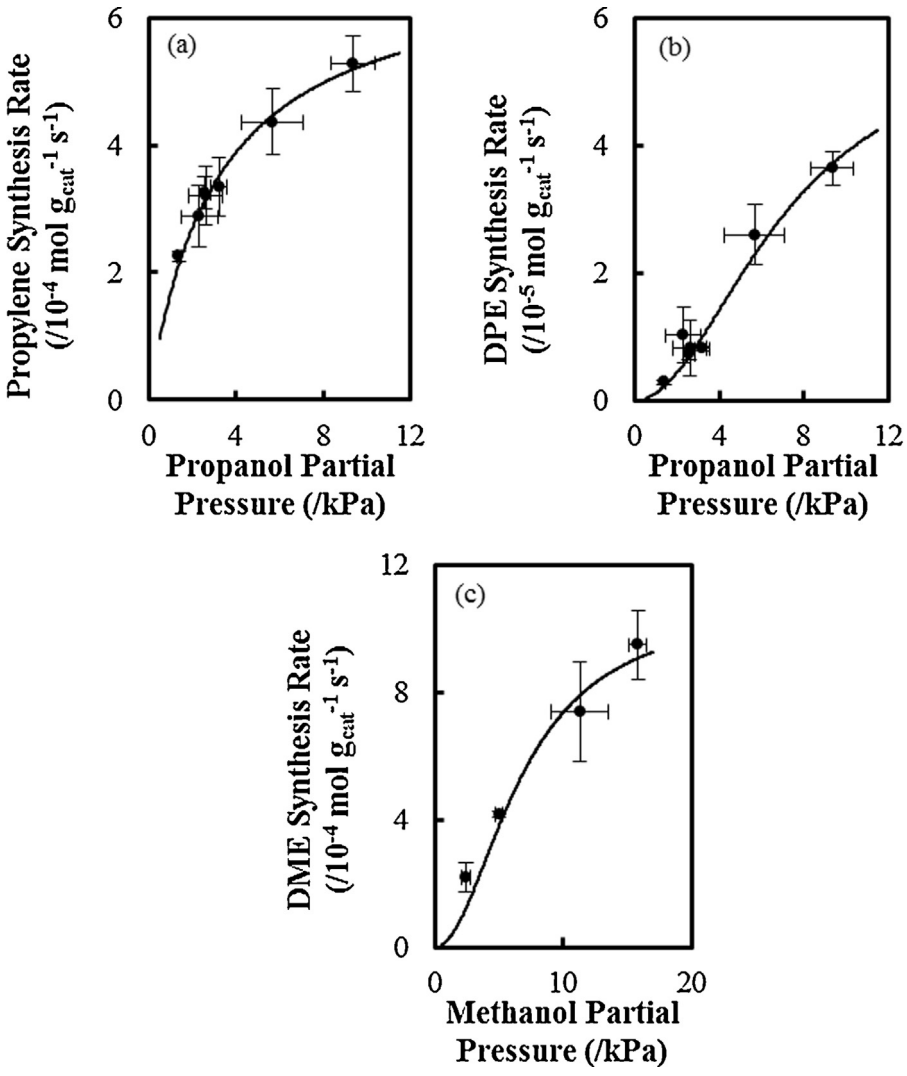

Fig. 1. (a) Propylene, (b) DPE, and (c) DME synthesis rates over 1.0 mg γ-Al_2O_3 (total volumetric flowrate = 9.9 cm^3 s^{-1}) at 623 K as a function of fed (a,b) 1-propanol and (c) methanol partial pressure with a co-feed of (a,b) 0.7 kPa or (c) 1.5 kPa of water. Solid lines show kinetic model fits to Eqs. (a) (12) and (b,c) (13).

parity, lag, and normal probability plots for the kinetic models for each reaction.

The rate of MPE hydration over γ-Al_2O_3 at 623 K, as defined in Eq. (1), is negligible in reference to experimental variance and uncertainties at water partial pressures below 2.1 kPa (Fig. 3). The calculated rates of 1-propanol dehydration at the effluent 1-propanol partial pressures were at least two orders of magnitude smaller than all other rates in Eqs. (1)–(3); therefore, the rates of 1-propanol conversion throughout the bed were neglected in this analysis. Methanol was co-fed to avoid concentration gradients of methanol across the packed bed that could affect the observed rate of the reaction of methanol and MPE to synthesize DME and 1-propanol. The average effluent pressure of 1-propanol was small (1.5 Pa) relative to the fed MPE (0.8 kPa) and methanol (0.2 kPa) partial pressures, the reactants of the remaining kinetically relevant reactions. Therefore, the rate of DPE synthesis from the reaction of MPE and 1-propanol, $r_{MPE+PrOH}$ was neglected in this analysis; if this rate was taken into account, it would lower the already negligible calculated hydration rate. The negligible ether hydration rates lead us to conclude that, at water partial pressures below 2.1 kPa, the measured rate of conversion of light ethers, such as DEE, are primarily a result of ether disproportion. The conclusion that ether disproportionation is the primary ether consumption pathway on γ-Al_2O_3 is consistent with the 1:1 stoichiometric production of ethanol and ethylene at low conversions from DEE conversion over γ-Al_2O_3 at 523–616 K observed previously by Knözinger and Köhne

Table 1
Kinetic parameters corresponding to models for unimolecular and bimolecular dehydration shown in Eqs. (12) and (13) for the synthesis of propylene, DPE, and DME from alcohol dehydration on γ-Al_2O_3 at 623 K estimated from the data presented in Figs. 1 and 2.

Propylene (Eq. (12))		Dipropyl Ether (Eq. (13))		Dimethyl Ether (Eq. (12))	
k_{olefin} ($/10^{-4}$ $mol_{C_2H_6}$ s^{-1} g^{-1})	K_{A1} (kPa^{-1})	k_{ether} ($/10^{-5}$ mol_{DPE} s^{-1} g^{-1})	$K_{A1}K_{A2}$ (kPa^{-2})	k_{ether} ($/10^{-4}$ mol_{DME} s^{-1} g^{-1})	$K_{A1}K_{A2}$ (kPa^{-2})
6.9 ± 0.9	0.32 ± 0.09	5.8 ± 1.5	0.020 ± 0.009	11 ± 2	0.022 ± 0.009

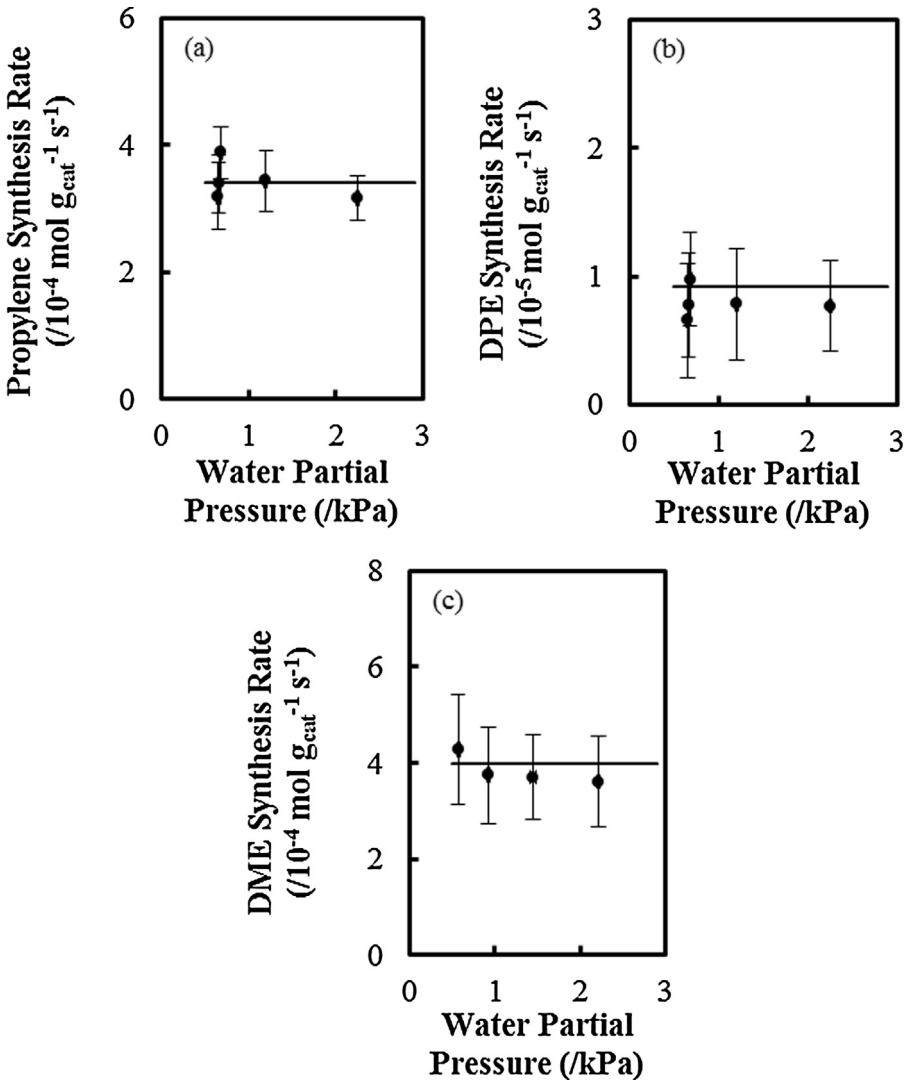

Fig. 2. (a) Propylene, (b) DPE, and (c) DME synthesis rates from the conversion of (a,b) 3.0 kPa of 1-propanol and (c) 5.2 kPa of methanol over 1.0 mg γ-Al_2O_3 (total volumetric flowrate = 9.9 cm^3 s^{-1}) at 623 K as a function of water partial pressure. Solid lines show model fits to Eqs. (a) (12) and (b,c) (13).

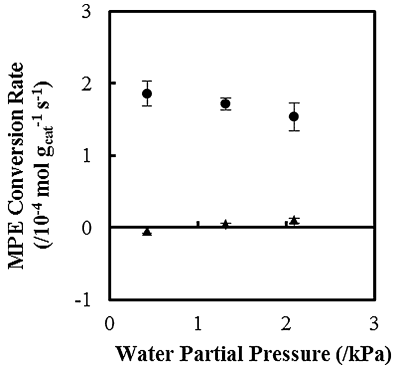

Fig. 3. The conversion rate of 0.8 kPa of MPE through (●) disproportionation and (▲) hydration on 1.0 mg of γ-Al_2O_3 at 623 K as a function of co-fed water partial pressure. A co-feed of 0.2 kPa of methanol was added to avoid methanol concentration gradients across the reactor.

as well as Morávek and Kraus [27,29]. The kinetic dominance of ether disproportionation at low water partial pressures (<2.1 kPa) allows for the evaluation of the kinetics of DEE disproportionation in absence of complications arising from multiple DEE conversion pathways.

3.2. Steady state kinetic measurements of DEE disproportionation

The rate of DEE disproportionation at 623 K possesses a DEE partial pressure order between 0 and 1, decreasing with increasing DEE partial pressure (going from 0.6 to 0.2 as DEE partial pressure is increased from 0.4 to 8.5 kPa; Fig. 4a). Additionally, DEE disproportionation rates decrease by a factor of 20% when the ethanol partial pressure is increased from 0.3 to 0.5 kPa (DEE pressure = 4.3 kPa), demonstrating that ethanol-derived surface species inhibit DEE conversion at 623 K (Fig. 4a). This observation is consistent with measured ethanol dehydration kinetics in which ethanol-derived surface species were observed to be a kinetically relevant species above 623 K [23]. As is the case with MPE disproportionation (Fig. 3) and ethanol dehydration [23] at 623 K, DEE disproportionation rates are independent of water partial pressure below 1.0 kPa of water (Fig. 4b), verifying that water-derived surface species are not stable on the catalytically active sites of γ-Al_2O_3 at 623 K.

A mechanism for the disproportionation of DEE that is consistent with the steady state kinetic measurements shown in Fig. 4 is presented in Scheme 2. In this mechanism, DEE first adsorbs onto an empty catalytic site on the γ-Al_2O_3 surface. The DEE then dissociates to form two C_2 surface species, likely two surface ethoxy species, one of them comprising a lattice oxygen atom. The surface

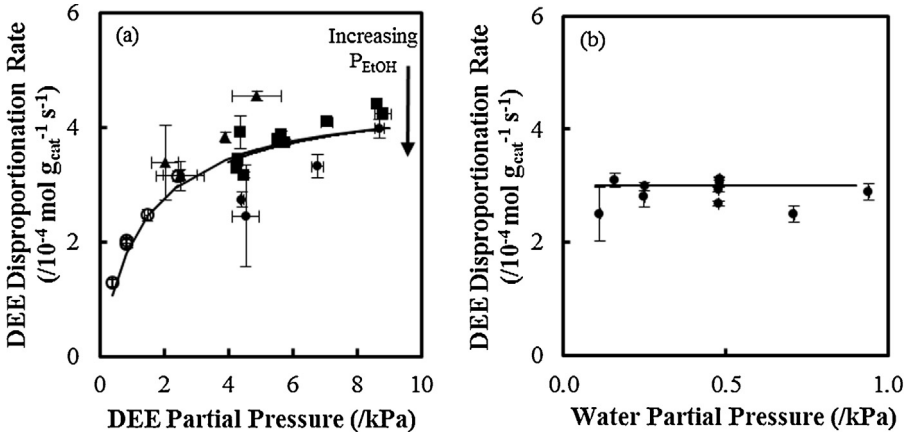

Fig. 4. DEE disproportionation rates over 1.0 mg of γ-Al_2O_3 at 623 K as a function of (a) DEE partial pressure with a 0.5 kPa water co-feed and (b) co-fed water partial pressure with a feed DEE partial pressure of 2.4 kPa. In the data presented in (a) ethanol was both independently fed and in the DEE feed solution as a stabilizing agent, the average total fed ethanol partial pressure was (○) 0.1 kPa, (▲) 0.2 kPa, (■) 0.3 kPa, and (●) 0.5 kPa. The solid lines show model fits to Eq. (14).

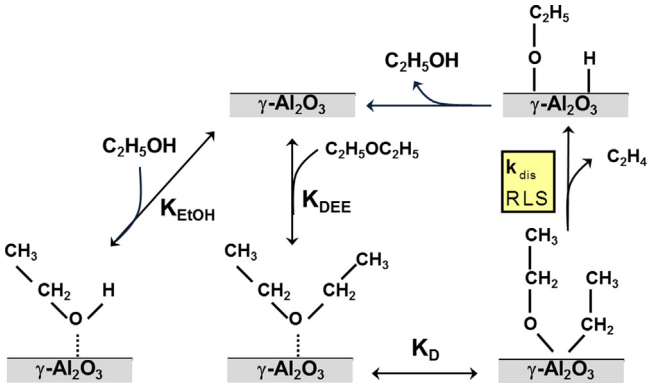

Scheme 2. The proposed mechanism for DEE disproportionation on γ-Al_2O_3.

ethoxy containing the lattice oxygen then undergoes decomposition via cleavage of the C_β—H and C—O bonds to form a gas phase ethylene molecule and a surface-bound hydrogen adatom in a manner analogous to the decomposition of ethoxy species in the postulated mechanism for unimolecular ethanol dehydration reported previously [22]. The surface-bound hydrogen adatom and the remaining surface-bound ethoxy species recombine to synthesize ethanol and regenerate the catalyst surface.

The rate-limiting step of the mechanism depicted in Scheme 2 is similar to that for ethylene synthesis from ethanol dehydration on γ-Al_2O_3 discussed in our previous reports [22,23]. In these reports, a primary kinetic isotope effect (KIE) for ethylene synthesis was only observed when the C—H bonds of the ethanol were deuterated (r_H/r_D = 2.4 at 488 K and r_H/r_D = 1.9 at 623 K), verifying that C—H bond cleavage, likely that of a C_β—H bond, was rate-limiting for ethylene synthesis. Similarly, Knözinger and Scheglila [11] measured a primary KIE for the dehydration of *tert*-, *sec*-, and *iso*-butanol only when the C_β—H bond of the reactant was deuterated. Considering the rate-limiting step for ethylene formation is the same for both ethanol dehydration and DEE disproportionation, the rate equation for DEE disproportionation, r_{dis}, shown in Eq. (14)

can be derived assuming that chemisorbed ethanol and surface ethoxy species formed from dissociated DEE are the prominent surface species on the active sites and are in quasi-equilibrium with gas phase ethanol and DEE.

$$r_{dis} = \frac{k_{dis}K_{DEE}K_D P_{DEE}}{1+K_{DEE}K_D P_{DEE}+K_{EtOH}P_{EtOH}} \quad (14)$$

Table 2
Kinetic parameters for DEE disproportionation on γ-Al_2O_3 at 623 K estimated using the model presented in Eq. (14) and the data presented in Fig. 4.

Parameter	k_{dis} (/10^{-4} mols^{-1}g^{-1})	$K_{DEE}K_D$ (kPa^{-1})	K_{EtOH} (kPa^{-1})
Value	4.6 ± 0.5	0.78 ± 0.32	0.22 ± 0.17

k_{dis} is the intrinsic rate constant for DEE disproportionation. K_{DEE} and K_{EtOH} signify the equilibrium constants of adsorption for DEE and ethanol, respectively. K_D is the equilibrium constant for dissociation of an adsorbed DEE molecule into two surface ethoxy groups, one containing an oxygen atom from the reactant molecule and another containing a lattice oxygen atom. P_{DEE} and P_{EtOH} respectively represent the partial pressures of DEE and ethanol. The values for the kinetic parameters k_{dis} and K_{DEE} of Eq. (14) were estimated from the data in Fig. 4 and are compiled in Table 2. The equilibrium constant for the adsorption of ethanol to form chemisorbed species that are reactive for ethylene synthesis from dehydration, K_{EtOH}, was evaluated previously (0.22 ± 0.17 kPa^{-1}) [23] and was held constant in the parameter estimation for DEE disproportionation (Eq. (14)). The solid line in Fig. 4 shows the fit of the kinetic model presented in Eq. (14). A statistical analysis of the residual errors of this kinetic model, including parity, lag, and normal probability plots, is presented in the supplementary information (Fig. S5).

The value for the intrinsic rate constant for DEE disproportionation, (4.6 ± 0.5) × 10^{-4} mol s^{-1} g^{-1}, is approximately a factor of two lower than the previously reported value for unimolecular dehydration of ethanol on γ-Al_2O_3 to form ethylene at 623 K, (9.4 ± 3.3) × 10^{-4} mol s^{-1} g^{-1} [23]. We postulate that the comparable values in the rate constants for these steps correspond to similarities in the proposed rate-limiting steps; in both reactions, the C_β—H bond of a C_2 surface species, postulated to be an ethoxy group, is cleaved in the rate-limiting step to form ethylene [22]. This result is supported by the previously mentioned DFT calculations of Christiansen et al. [30] in which the calculated barrier for DEE disproportionation (38 kcal mol^{-1}) was nearly equivalent to that of unimolecular ethanol dehydration (37 kcal mol^{-1}).

The form of the rate equation presented in Eq. (14) is consistent with an alternative mechanism in which adsorbed DEE, rather than ethoxy groups formed by DEE dissociation, directly disproportionates in the rate-limiting step to form ethylene, a surface ethoxy group, and a surface hydrogen adatom. The direct decomposition of ethers as well as alcohols was proposed by Roy et al. [19] and Christiansen et al. [30,39] as the reaction pathway with

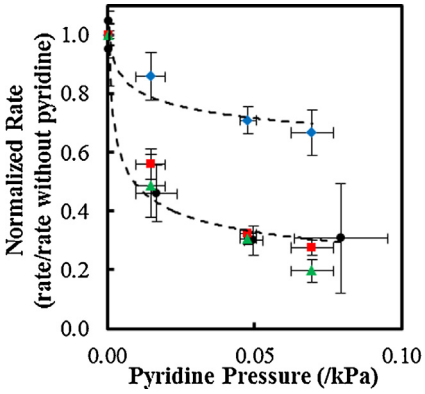

Fig. 5. The rate of (●) DEE disproportionation from the conversion of 1.4 kPa of DEE as well as the independently evaluated (■) ethylene, (◆) DEE, and (▲) acetaldehyde synthesis rates from the conversion of 3.5 kPa of ethanol with a 1.3 kPa water co-feed on γ-Al_2O_3 at 623 K normalized to their rates in absence of pyridine as a function of co-fed pyridine partial pressure. The dashed lines serve as a guide for the eye.

the lowest calculated (density functional theory; PW 91) activation energies (38 and 37 kcal mol^{-1} for DEE and ethanol, respectively). The direct decomposition of adsorbed ethanol, rather than the decomposition of ethoxy groups, was also discussed as an alternative mechanism for unimolecular ethanol dehydration in previous reports [22–24], demonstrating that the concluded similarities in the rate-limiting steps of DEE disproportionation and unimolecular ethanol dehydration are still valid with the alternative mechanism. Both potential mechanisms are kinetically equivalent; thus, the functional form of Eq. (14), the kinetic parameters presented in Table 2, and the site requirement analysis discussed in Section 3.3 would be unaffected by the choice of the modeled mechanism.

3.3. DEE disproportionation site requirements and density on γ-Al_2O_3

In previous investigations, the degree of inhibition of measured steady state reaction rates by pyridine was used to probe the site requirements of ethanol dehydration and dehydrogenation on γ-Al_2O_3. Specifically, pyridine inhibited DEE synthesis to a lesser extent than ethylene or acetaldehyde synthesis from the conversion of ethanol, demonstrating that unimolecular reactions of ethanol occur on a separate pool of catalytic sites from bimolecular ethanol dehydration [22,23].

The rate of DEE disproportionation at 623 K is inhibited by pyridine to the same extent as ethylene and acetaldehyde synthesis from ethanol dehydration and dehydrogenation and to a greater extent than DEE synthesis from bimolecular ethanol dehydration (Fig. 5). This result demonstrates that DEE disproportionation occurs on catalytic sites that adsorb pyridine equivalently to those that are active for unimolecular ethanol dehydration and dehydrogenation, revealing the similar site requirements for these chemistries. Furthermore, the different extents of inhibition of DEE synthesis and disproportionation by pyridine verifies that the pool of catalytic sites responsible for bimolecular ethanol dehydration and, thus, its reverse reaction DEE hydration is not equivalent to the pool responsible for DEE disproportionation. The similar site requirements and rate constants for ethylene synthesis from ethanol dehydration and DEE disproportionation reinforces the mechanism proposed in Scheme 2 in which ethylene is formed in a rate-limiting step that involves the cleavage of a C_β—H bond of a surface ethoxy species as was the case for unimolecular ethanol dehydration [22].

Previously, transient in-situ titrations of ethanol dehydration over γ-Al_2O_3 at 623 K with pyridine estimated the surface density

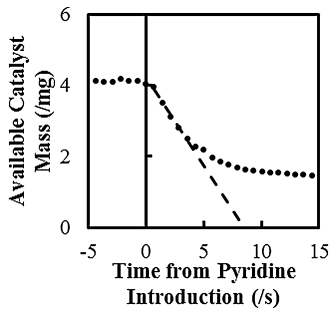

Fig. 6. Catalyst mass available for the disproportionation of 1.5 kPa of DEE over 0.005 g of γ-Al_2O_3 at 623 K (total gas flowrate = 9.9 $cm^3\ s^{-1}$) as a function of time after the introduction of 0.05 kPa of pyridine to the feed. The dashed line shows the linear extrapolation used to determine the pyridine uptake necessary to completely deactivate the rate of DEE disproportionation.

Table 3
Estimated pyridine surface density necessary to completely deactivate the sites for DEE disproportionation over γ-Al_2O_3 at 623 K determined from in-situ pyridine titrations at different catalyst loadings and pyridine partial pressures. The reported errors are 95% confidence intervals evaluated using independent titrations.

Pyridine uptake (/10^{-5} mol g^{-1})	Catalyst mass	
Pyridine pressure	0.010 g	0.005 g
0.02 kPa	7.7 ± 0.5	9.5 ± 1.5
0.05 kPa	7.2 ± 0.5	9.0 ± 1.1

of catalytic sites responsible for ethylene synthesis to be 0.2 sites nm^{-2} [23]. The density of active sites was evaluated by analyzing the decay in available catalyst mass for DEE disproportionation after pyridine was introduced to the reactor feed using measured reactor effluent compositions, Eq. (14), and previously evaluated kinetics for ethanol dehydration [23]. To estimate the catalytic site density from this transient deactivation profile, we assume that initially (far from equilibrium) each molecule of pyridine that enters uniquely adsorbs onto one of the catalytic sites and that every catalytic site for DEE disproportionation is equivalent. We then determine the total pyridine uptake that would completely shut down DEE disproportionation by extrapolating the initial linear decay of the calculated available catalyst mass upon introduction of pyridine to the feed stream (example in Fig. 6). Using this technique at different pyridine pressures and catalyst loadings, the average pyridine uptake necessary to completely shut down DEE disproportionation on γ-Al_2O_3 at 623 K was determined to be $(8.4 \pm 0.5) \times 10^{-5}$ mol g_{cat}^{-1}, corresponding to 0.3 sites nm^{-2} (Table 3). This estimation of site density represents an upper bound because pyridine could adsorb onto non-active sites during the titration. The comparable estimated catalytic site densities for DEE disproportionation and ethylene synthesis from ethanol dehydration (0.3 and 0.2 sites nm^{-2}, respectively) reinforce the conclusion that the site requirements of these two reactions are similar [23]. The nonequivalent nature of the catalytic sites that catalyze DEE disproportionation and those that are active for DEE synthesis from ethanol dehydration on γ-Al_2O_3 is illustrated by the ~6-fold difference in estimated catalytic site densities at 623 K (0.3 and 1.8 sites nm^{-2} for DEE disproportionation and synthesis, respectively) [23].

Christiansen et al. [39] calculated that energy barriers for ethylene synthesis from ethanol dehydration differ among the facets of γ-Al_2O_3 (37, 30, and 28 kcal mol^{-1} for the (1 0 0), (1 1 0), and (1 1 1) facets, respectively) while the activation energies for DEE synthesis did not differ substantially (35, 34, and 32 kcal mol^{-1} for the (1 0 0), (1 1 0), and (1 1 1) facets, respectively). The discrepancy in the calculated activation energies for unimolecular and bimolecular alcohol dehydration on different facets of γ-Al_2O_3 is consistent with our conclusion that at least two non-equivalent pools of catalytic sites exist on the γ-Al_2O_3 surface. These calculations allow

us to postulate the identity of the active surfaces for the two pools of the catalytic sites. We propose that unimolecular reactions of ethanol and DEE occur preferentially on higher-indexed facets of γ-Al_2O_3, (1 1 0) and (1 1 1), while bimolecular dehydration and ether hydration can occur on each of the three prominent facets ((1 0 0), (1 1 0), and (1 1 1)), reflected by our measured ~6-fold difference in catalytic site densities for DEE synthesis from ethanol dehydration and DEE disproportionation. Electron diffraction patterns and transmission electron microscopy images of plate-like γ-Al_2O_3 particles synthesized by Kovarik et al. [40] demonstrate that the (1 1 0) and (1 1 1) facets dominate the external surfaces of these particles while the surfaces in the particle pores primarily comprise the (1 0 0) and (1 1 1) facets. Furthermore, the authors concluded, based on observed surface reconstructions, that the surface energies of these exposed facets increase in the following manner: (1 0 0), (1 1 1), and (1 1 0) [40]. We propose that pyridine preferentially adsorbs onto the facets with higher surface energies, (1 1 0) and (1 1 1). Therefore, the observation that ethylene and acetaldehyde synthesis from ethanol dehydration and DEE disproportionation are inhibited by pyridine to a greater extent than DEE synthesis (Fig. 5) is consistent with our postulate that only these higher energy surfaces catalyze unimolecular reactions on γ-Al_2O_3 while bimolecular reactions can also be activated by the (1 0 0) surface. The postulate that multiple pools of catalytic sites exist on γ-Al_2O_3 is consistent with the microkinetic model of ethanol dehydration developed by Christiansen et al. [39] in which both DEE and ethylene synthesis could not be described with complete accuracy using only the (1 1 1) facet. Based on our postulate, we predict that transitional alumina phases which predominantly feature the (1 1 1) and (1 1 0) facets, such as η- or θ-Al_2O_3 [41], will produce ethylene with higher selectivity than γ-Al_2O_3. This prediction will be the subject of future investigations.

One complication that may alter our prediction is the stability of surface hydroxyl groups on each surface facet for each alumina. In a previous report [23], we determined that the density of catalytic sites that catalyze DEE synthesis from ethanol dehydration increased from 0.1 to 1.8 sites nm^{-2} as the reaction temperature was increased from 488 to 623 K. We postulated that this increase in site density was a result of a lower density of surface hydroxyl groups at higher reaction temperatures. DFT calculations (PW91) by Digne et al. [32,42] determined that the density of surface hydroxyl groups on the (1 0 0) and (1 1 0) facets of γ-Al_2O_3 at 488 K was 8.8 and 11.8 OH nm^{-2}, respectively; At 623 K, the calculated density decreased to 0 and 8.9 OH nm^{-2}, respectively, supporting our explanation for the increased site density at higher temperatures.

The derived kinetics and site requirements for DEE disproportionation in this report describe one of the necessary DEE conversion pathways to model the reaction network of ethanol dehydration on γ-Al_2O_3 to selectively form ethylene. These DEE conversion pathways explain the negligible DEE yields from ethanol dehydration on γ-Al_2O_3 at very high conversions (>99%) at 623 K observed by Phung et al. [26] as well as our studies shown in Fig. S1. The reported kinetic model for DEE disproportionation and those derived previously for ethanol dehydration [22–24] comprise a mechanistic picture capable of rigorously describing the conversion pathways of ethanol on γ-Al_2O_3.

4. Conclusions

Steady state kinetic measurements of MPE conversion on γ-Al_2O_3 at 623 K confirm that ether hydration rates are negligible compared to ether disproportionation rates at water partial pressures below 2.0 kPa. Measured DEE disproportionation rates possess a DEE reaction order between 0 and 1 (between 0.4 and 8.5 kPa of DEE) and are independent of co-fed water partial pressure. A mechanism in which the rate-limiting step is ethylene formation from a surface ethoxy group and surface-bound ethanol monomers and DEE-derived ethoxy groups primarily cover the catalytic sites describes the measured DEE rates. The estimated intrinsic rate constants for DEE disproportionation and ethylene synthesis from ethanol dehydration [23] on γ-Al_2O_3 are within a factor of two, demonstrating the similarities in the rate-limiting steps of these reactions. DEE disproportionation rates are inhibited by pyridine to the same extent as ethylene synthesis rates from ethanol dehydration on γ-Al_2O_3 and to a greater extent than DEE synthesis rates from bimolecular dehydration. The estimated density of catalytic sites responsible for DEE disproportionation (0.3 sites nm^{-2}) is comparable to that of ethylene synthesis from ethanol dehydration (0.2 sites nm^{-2}). These results verify that (i) unimolecular dehydration of ethanol and DEE disproportionation possess similar site requirements, supporting the common rate-limiting steps conjectured for each reaction, and (ii) bimolecular ethanol dehydration and DEE disproportionation occur on non-equivalent catalytic sites.

Acknowledgements

We would like to thank The Dow Chemical Company and the University of Minnesota Doctoral Dissertation Fellowship for their financial support. We would also like to thank Mr. Marcello Herrera and Mr. Minje Kang for helpful technical discussions.

Appendix A. Supplementary data

Supplementary data associated with this article can be found, in the online version, at http://dx.doi.org/10.1016/j.apcata.2015.06.008

References

[1] B.C. Lippens, J.H. De Boer, Acta Crystallogr. 17 (1964) 1312–1321.
[2] R.C.T. Slade, J.C. Southern, I.M. Thompson, J. Mater. Chem. 1 (1991) 563–568.
[3] Y. Cesteros, P. Salagre, F. Medina, J.E. Sueiras, Chem. Mater. 11 (1999) 123–129.
[4] Industrial minerals & rocks, in: J.E. Kogel, N.C. Trivedi, J.M. Barker, S.T. Krukowski (Eds.), Society for Mining, Metallurgy, and Exploration, 7th ed., Englewood, CO, 2006.
[5] I. Chorkendorff, J.W. Niemantsverdriet, Concepts of Modern Catalysis and Kinetics, Wiley-VCH, 2007, pp. 193–195.
[6] J.H. Kwak, C.H.F. Peden, J. Szanyi, J. Phys. Chem. C 115 (2011) 12575–12579.
[7] P. Kostestkyy, J. Yu, R.J. Gorte, G. Mpourmpakis, Catal. Sci. Technol. 4 (2014) 3861–3869.
[8] H. Knözinger, Angew. Chem. Int. Ed. 7 (1968) 791–805.
[9] H. Knözinger, H. Bühl, E. Ress, J. Catal. 12 (1968) 121–128.
[10] H. Knözinger, A. Scheglila, A.M. Watson, J. Phys. Chem. 72 (1968) 2770–2774.
[11] H. Knözinger, A. Scheglila, J. Catal. 17 (1970) 252–263.
[12] H. Knözinger, H. Bühl, K. Kochloefl, J. Catal. 24 (1972) 57–68.
[13] E.C. DeCanio, V.P. Nero, J.W. Bruno, J. Catal. 135 (1992) 444–457.
[14] B.C. Shi, B.H. Davis, J. Catal. 157 (1995) 359–367.
[15] P.A. Clayborne, T.C. Nelson, T.C. DeVore, Appl. Catal. A 257 (2004) 225–233.
[16] J.H. Kwak, J.Z. Hu, D.H. Kim, J. Szanyi, C.H.F. Peden, J.Catal. 251 (2007) 189–194.
[17] H.A. Dabbagh, M. Zamani, B.H. Davis, J. Mol. Catal. A: Chem. 333 (2010) 54–68.
[18] J. Kwak, D. Mei, C.F. Peden, R. Rousseau, J. Szanyi, Catal. Lett. 141 (2011) 649–655.
[19] S. Roy, G. Mpourmpakis, D. Hong, D.G. Vlachos, A. Bhan, R.J. Gorte, ACS Catal. 2 (2012) 1846–1853.
[20] R.S. Schiffino, R.P. Merrill, J. Phys. Chem. 97 (1993) 6425–6435.
[21] V.A. Matyshak, L.A. Berezina, O.N. Sil'chenkova, V.F. Tret'yakov, G.I. Lin, A.Y. Rozovskii, Kinet. Catal. 50 (2009) 111–121.
[22] J.F. DeWilde, H. Chiang, D.A. Hickman, C.R. Ho, A. Bhan, ACS Catal. 3 (2013) 798–807.
[23] J.F. DeWilde, C.J. Czopinski, A. Bhan, ACS Catal. 4 (2014) 4425–4433.
[24] M. Kang, J.F. DeWilde, A. Bhan, ACS Catal. 5 (2015) 602–612.
[25] L. de Mourgues, F. Peyron, Y. Trambouze, M. Prettre, J. Catal. 7 (1967) 117–125.
[26] T.K. Phung, A. Lagazzo, M.Á. Rivero Crespo, V. Sánchez Escribano, G. Busca, J. Catal. 311 (2014) 102–113.
[27] H. Knözinger, R. Köhne, J. Catal. 5 (1966) 264–270.
[28] T.K. Phung, G. Busca, Chem. Eng. J. 272 (2015) 92–101.
[29] V. Morávek, M. Kraus, J. Catal. 87 (1984) 452–460.
[30] M.A. Christiansen, G. Mpourmpakis, D.G. Vlachos, ACS Catal. 3 (2013) 1965–1975.

[31] R. Wischert, P. Laurent, C. Copéret, F. Delbecq, P. Sautet, J. Am. Chem. Soc. 134 (2012) 14430–14449.
[32] M. Digne, P. Sautet, P. Raybaud, P. Euzen, H. Toulhoat, J. Catal. 226 (2004) 54–68.
[33] B.A. Hendriksen, D.R. Pearce, R. Rudham, J. Catal. 24 (1972) 82–87.
[34] C. Morterra, G. Magnacca, Catal. Today 27 (1996) 497–532.
[35] E.P. Parry, J. Catal. 2 (1963) 371–379.
[36] J.A. Ripmeester, J. Am. Chem. Soc. 105 (1983) 2925–2927.
[37] A. Zecchina, E.E. Platero, E.O. Areán, J. Catal. 107 (1987) 244–247.
[38] R. Wischert, P. Florian, C. Copéret, D. Massiot, P. Sautet, J. Phys. Chem. C 118 (2014) 15292–15299.
[39] M.A. Christiansen, G. Mpourmpakis, D.G. Vlachos, J. Catal. 323 (2015) 121.
[40] L. Kovarik, A. Genc, C. Wang, A. Qiu, C.H.F. Peden, J. Szanyi, J.H. Kwak, J. Phys. Chem. C 117 (2013) 179–186.
[41] G. Busca, in: Friederike C. Jentoft (Ed.), Advances in Catalysis, Academic Press, 2014, pp. 319.
[42] P. Digne, P. Sautet, P. Euzen, H. Toulhoat, J. Catal. 211 (2002) 1–5.